MUONS AND NEUTRINOS

T. STANEV*
Physics Department, University of Wisconsin
Madison, Wisconsin 53706
and
Bartol Research Foundation, University of Delaware
Newark, Delaware 19716

INTRODUCTION

This conference comes at a time of major experimental developments in the underground physics. The first generation of large and precise detectors, some initially dedicated to search for nucleon decay, has accumulated significant statistics on neutrinos and high-energy muons. A second generation of even better and bigger detectors are already in operation or in advanced construction stage. The present set of experimental data on muon groups and neutrinos is qualitatively better than the one we had several years ago and the expectations for the following years are high.

The interpretation of these results, however, is far from complete. Most, if not all, of the particles observed underground are produced in cascades generated in the atmosphere by primary cosmic rays. Thus the data interpretation involves complex and time-consuming calculations of the cascade development, propagation to the detector through the surrounding rock and the detector response, which are not always consistently performed for each detector. The importance of such calculations increases with the increasing complexity of the investigated phenomenon and is, for example, crucial for the interpretation of muon groups.

The chemical composition of the cosmic-ray flux and the characteristics of the inelastic interactions in the atmosphere, two main assumptions in cascade calculations, vary widely from author or author. And while the composition is often the subject of the investigation, I do not see at the present time reasons for a drastic change of the interaction models from what is observed at accelerators. The $\bar{p}p$ collider at CERN, which works at equivalent laboratory energies up to 4.3×10^5 GeV, has established certain deviations from Feynman scaling such as energy-dependent cross section, $\ell n^2 s$ term in the average charged multiplicity and broadening of the multiplicity distribution with the energy, but has not found evidence for serious scaling violation in the fragmentation region.[1] The measurements extend to only $x \cong 0.05$, but

* On leave of absence from the Institute for Nuclear Research and Nuclear Energy, Sofia 1784, Bulgaria.

the total amount of energy released in such particles can be used[2] to estimate the behavior at higher x. Some uncertainty in the interaction model is introduced by the fact that the atmosphere provides a nuclear target and the transformation from pp to pN interactions is model-dependent. There is, however, enough lower-energy (up to 400 GeV) data, which can guide the required modification of the interaction models for hadron interactions on light nuclei.

In this talk I shall concentrate on three topics, which not only have significant scientific importance, but were also discussed at this conference by independent groups. They are:

- composition studies with underground muon groups,
- neutrino detection,
- expected extraterrestrial neutrino fluxes.

INVESTIGATION OF THE PRIMARY COSMIC-RAY COMPOSITION WITH UNDERGROUND MUON GROUPS

The studies of the chemical composition of the cosmic-ray flux at energy $> 10^{14}$ eV have produced one of the most contradictory sets of results in the whole field. The fluxes at such energies are low enough not to permit statistically adequate direct measurement and the indirect evaluations from cascade properties such as depth of maximum and muon-to-electron ratio did not allow unique interpretation and produced vastly different results.[3]

It does not seem possible from air shower data to judge even such distinctly different models as the proton-dominated light composition, suggested by J. Linsley[4] and the more conservative composition derived by G. B. Yodh and collaborators[5] from studies of delayed hadrons in air showers, which contains an increasing with the energy fraction of heavy nuclei.

The sensitivity of the muon groups to the composition arises from the different muon yields from nuclei of different mass and the same total energy. Figure 1 shows the average number of muons produced at depth 4 km.w.e. (effective $E_\mu \geq 2.1$ TeV) by protons and iron nuclei. The yield of an iron nucleus is zero before the energy per nucleon exceeds E_μ and rises faster than the proton one until an asymptotic behavior is established. The following features of the production of high-energy muons have been established in numerous Monte Carlo studies:[6]

1. $N_\mu(> E_\mu) = \frac{kA\sec 0}{E_\mu}\left(\frac{E_\mu}{E_0/A}\right)^\alpha\left(1-\frac{E_\mu}{E_0/A}\right)^\beta$ is the Elbert's formula relating the muon yield to the primary energy and mass. The sec0 dependence of the yield holds up to 60°.

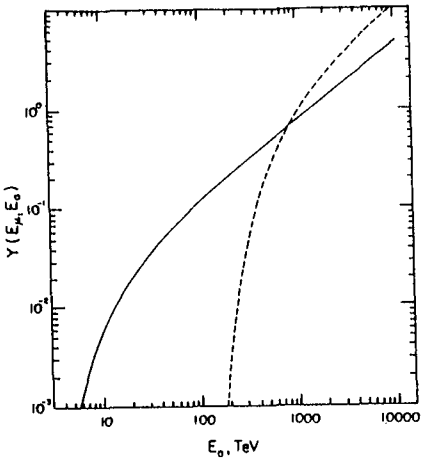

Fig. 1. Muon yields from primary protons (solid line) and iron nuclei (dash line) at depth of 4 km.w.e.

2. The muon multiplicity distribution in a single shower is very close to and can be approximated with a Poissonian.

3. The lateral distribution of muons depends on the primary energy per nucleon E_0/A and the cross section, which leads to an explicit A dependence.

The knowledge of the lateral distribution is very important in view of the fact that most detectors are not much bigger than the average muon radius and thus suffer from confinement problems. The detected number of muons is only a fraction of the total multiplicity of the muon shower, which depends on the exact shape and resolution of the detector. The detection efficiency cannot be accounted for without extensive Monte Carlo study.

Three experimental groups presented results on the primary composition from observation of muon groups. The NUSEX group [OG 5.1-5] compares the observed muon multiplicity distribution (Fig. 2) with predictions for compositions, characterized by different spectral indexes of the iron component. The plotted prediction lines account for the detection efficiency and the slant depth variation with the zenith and azimuthal angle of the event.

The conclusion from the experiment is that the spectral index of the iron component, which fits the data best, is 2.7 and data do not agree with iron spectrum flatter than $E^{-2.6}$.

The Frejus group [HE 5.1-1] shows its first results on muon groups. This detector is impressive in both size and resolution and has collected significant statistics in a short time. Cascade calculations have indicated to the Frejus group that the ratio of events with $N_\mu \geq 7$ to $N_\mu = 4$, 5 and 6 is a good measure of the composition. The experimentally measured ratio is $\frac{N(\geq 7)}{N(4+5+6)} = 0.14 \pm 0.04$, which is in good agreement with a proton-dominated composition.

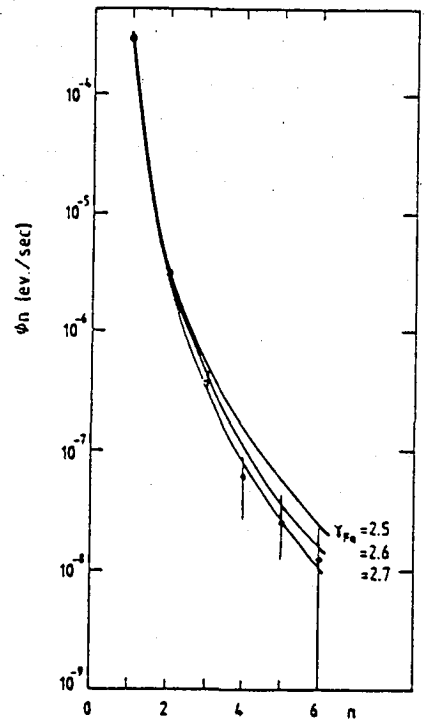

Fig. 2. Comparison of NUSEX rate of muon groups of multiplicity n to predictions from compositions with different spectral index for iron.

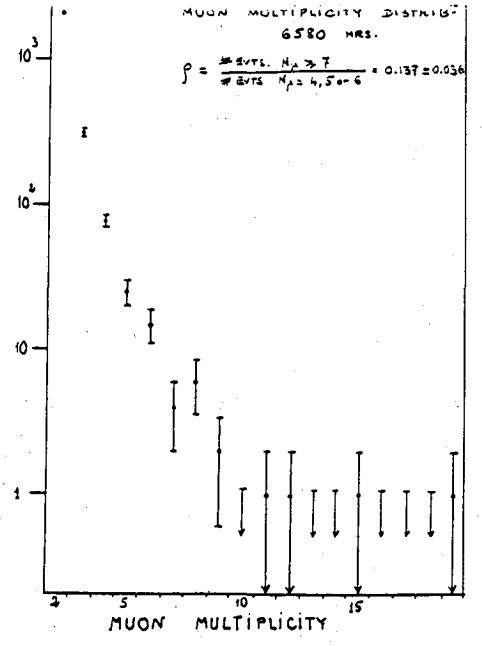

Fig. 3. Muon multiplicity distribution measured at Frejus.

The Baksan group has used two methods to derive the composition. The first one is similar to the approaches of the two other groups [HE 5.5-12]. Figure 4 shows the multiplicity distribution in the detector compared with predictions for pure compositions of different A (solid lines) and two composition models. A light energy-independent composition with $\langle A \rangle = 3.5$ best fits the data. $\langle A \rangle = \sum \beta_i A_i^2 / \sum \beta_i A_i$, where β_i is the fraction of nuclei with mass A_i on *E/nucleon* basis.

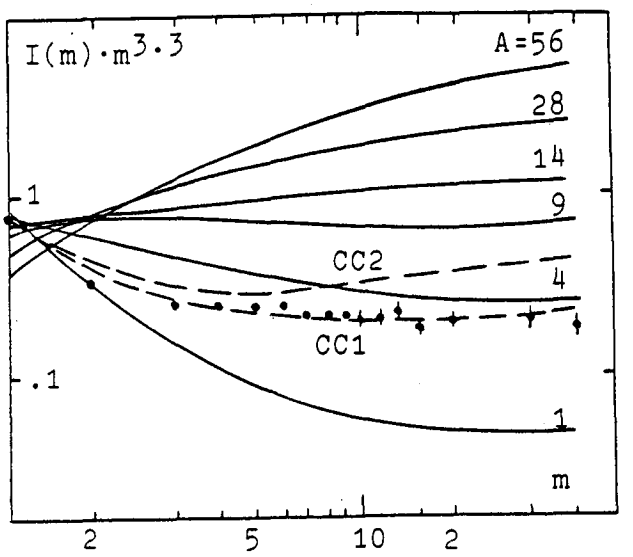

Fig. 4. Comparison of Baksan multiplicity distribution with predictions from pure (solid lines) and mixed compositions.

Note that because of the relatively shallow and large detector ($E_\mu > 0.22$ TeV) the observed multiplicities reach very high values.

The second approach is more interesting, because it involves an estimate of the primary energy [HE 5.1-13]. It is based on a calculated relation of the energy of the muon-induced showers in the detector to the primary energy per nucleon, which fits some other properties of the detected muon groups.

Figure 5 shows the observed dependence of the muon multiplicity N_μ on the primary energy E_0/A estimated through the energy of muon-induced showers in the detector. Curve 2 corresponds to a composition with $\langle A \rangle = 3.5$ and curve 3, which seems to fit data quite well, has $\langle A \rangle = 4.5$.

The conclusion from both approaches is that the primary composition does not change with energy and is dominated by protons up to 10^{15} eV.

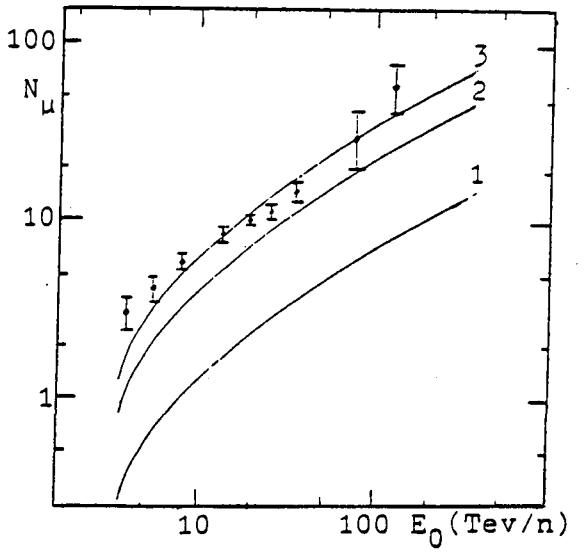

Fig. 5. Muon multiplicity at Baksan *vs.* the primary energy per nucleon. Curves correspond to compositions with $\langle A \rangle = 1$, 3.5 and 4.5.

The conclusions of all groups seem to agree with each other, although the results are expressed in different terms, and do not cover the same energy range. It would be helpful to compare the conclusions quantitatively with each other.

All conclusions are drawn from the fact that the heavy nuclei are more efficient in muon production than protons. The asymptotic behavior of the muon yield is

$$N_\mu(> E_\mu) = \left(\frac{k}{E_\mu}\right) A \left(\frac{A E_\mu}{E_0}\right)^{-0.78} \propto A^{\frac{1}{4}}$$

for equal zenith angle θ and muon energy E_μ. Since $A^{\frac{1}{4}}$ is a slowly increasing function of A, the sensitivity is not very big even for the asymptotic region, which is only partially examined in the experiments.

It seems reasonable to use as a common representation of all composition models one very simple parameter $R = \frac{L}{H}$, which is the ratio of the protons and α particles in a composition to all heavier nuclei. For energy-independent compositions $R = \text{const}$ and specifically $R \cong 2$ for the region where direct measurements are available. The energy-dependent compositions of Refs. 4 and 5 have the following R values at total energy 10^5 and 10^6 GeV:

Model	10^5 GeV	10^6 GeV
JL (Ref. 4)	1.89	2.85
MDII (Ref. 5)	0.74	0.34

Let us now calculate R for the compositions which best fit the experimental data. The two compositions favored by the Baksan results give $R = 1.7$ ($\langle A \rangle = 3.5$) and $R = 1.1$ ($\langle A \rangle = 4.5$). The only serious criticism I have of this experiment is that the interpretation does not account for the mass dependence of the muon lateral spread. The average muon spread used in the analysis is $\approx$ 13 m for vertical muons of $E = 0.22$ TeV, comparable to the dimensions of the detector, which is obviously not free from containment problems. The bigger lateral spread of iron showers might make the detector less efficient for their detection and decrease its sensitivity to composition.

The NUSEX result translates only into a limit $R \geq 0.7$. The reason is that the reference composition is already very heavy and the addition of more iron nuclei does not change significantly its basic property. The heavy reference composition also explains the low sensitivity to the iron fraction, which is obvious from Fig. 2. Despite the containment problems, the data set of NUSEX is one of the best available and certainly deserves a new analysis and comparison with lighter composition models.

The Frejus data give $R \lesssim 2$. The data set is relatively free from containment problems, but the presented interpretation has to be considered preliminary. I am not convinced that muon multiplicities $N_\mu \geq 7$ and $N_\mu = 4$, 5 and 6 reflect different components of the primary cosmic ray flux. Particularly the lower multiplicity group invevitably contains an admixture of events, generated by heavy primaries. It would probably be better to compare the multiplicity distribution with predictions of different models. Due to its big dimensions and excellent resolution, the Frejus detector is perfect for investigation of muon-induced showers. An attempt to estimate the primary energy from the energy released in the detector, in Baksan fashion, might give an additional handle on the composition problem.

Formally the papers presented at the Conference limit the value of our simple parameter $0.7 < R \leq 2$, an uncertainty not as bad as the spread of the values derived from different air shower properties. The existence of new large and precise detectors, such as Frejus and Homestake, which can collect statistics at a fast rate supports an optimistic view that with proper efforts in data analysis and interpretation the value of R will soon be determined with a reasonable precision of approximately 0.2 from measurements of underground muon groups.

NEUTRINO DETECTION

The worldwide statistics of neutrinos has been steadily growing in recent years. Table I shows the number of contained neutrino events in different detectors. Contained events are produced by neutrino interactions in the detector and the requirement for full containment is that all resulting tracks, as well as the vertex, are confined to the detector volume. Stars denote results, discussed at this conference.

Table I. Worldwide statistics on contained ν events, including nucleon decay candidates.

Experiment	Full containment	Vertex containment
IMB*[HE 5.3-7]	401	
KAMIOKANDE	107	
NUSEX*[HE 6.2-6]	32	
Frejus* Not in printed paper	13	21
KGF* Not in printed paper	19	40

Because of containment and flux restrictions, such events are produced by neutrinos of energy less than several GeV. The rate of such events can be calculated as

$$\text{Rate} = \sum_{i} \int_{E_i} \int_{E_\nu} dE_i \, dE_\nu \, \frac{dN_\nu}{dE_\nu} \, \frac{d\sigma}{dE_i} \, \epsilon_i(E_i) \, ,$$

where dN_ν/dE_ν is the neutrino flux, which we assume consists of atmospheric neutrinos only, $\frac{d\sigma_i}{dE_i}$ is the cross section for production of the i particle in a neutrino interaction and $\epsilon_i(E_i)$ is the energy-dependent detection efficiency for the i particle.

The atmospheric neutrino flux in the energy range responsible for contained events has been calculated by several authors.[7] The most recent calculation takes into account both the temporal and location variation of the neutrino flux.

The temporal variation is due to the solar modulation of the primary cosmic-ray flux and thus follows (with some delay) the 11-year variation of solar activity. Maximum flux is achieved about $1\frac{1}{2}$ years after solar minimum.

The cosmic-ray flux is further modulated in interaction with the geomagnetic field. Penetration through the field around the magnetic poles requires

less momentum than around the magnetic equator, so that the geomagnetic cut-off varies from a fraction to several tens of GV. Integrated over all zenith and azimuthal angles the influence of the geomagnetic field not only produces different fluxes at different experimental locations, but also affects the angular distribution of neutrinos at every given location.

Figure 6 shows the angular distribution of neutrinos with three different energies, calculated as in Ref. 7(e) for the location of the IMB experiment. While the angular distribution of the lower energy (0.2–0.4 GeV) neutrinos is very strongly affected by the geomagnetic field, its influence is negligible for $E_\nu > 2$ GeV. At higher energy the angular spread is only due to the different atmospheric thickness and structure at different angles.

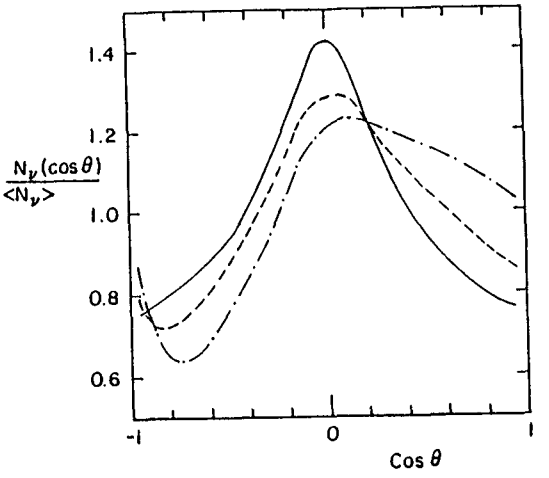

Fig. 6. Neutrino angular distribution at the site of the IMB experiment. Curves are for neutrinos of energy 0.2–0.4 GeV (dot-dash), 0.8–1 GeV (dash) and 2–3 GeV.

The cross sections in the energy range of interest here are well known for neutrino-nucleon scattering. All experiments, however, have nuclear targets, ranging from water to iron. Neutrino-nucleus cross sections are not well known and they induce an additional uncertainty in the calculated rates. As far as the majority of data on neutrinos of $E > 300$ MeV, however, this uncertainty is not very large, because in this range the nuclear cross sections are not expected to deviate very much from the cross section on free nucleons.

The detector response to the products of the neutrino interactions is studied at best by direct calibration in an accelerator beam (which was done for a fraction of the NUSEX detector) or by an extensive Monte Carlo study of the detector, as performed by the other groups.

The IMB collaboration operates an extremely large water Cherenkov detector with fiducial volume of 3.3 kt. Data from 420 days of running time has been analyzed, which gives a total exposure of 3.8 kt.yr. During that time 401 contained neutrino events have been observed, which with an overall efficiency of 0.80 gives a rate of 132 ν/kt.yr. Figure 7 shows a comparison of the experimentally observed neutrino energy spectrum in single-prong events[8] with a theoretical prediction, which combines the flux calculation of Ref. 7(e), averaged over all angles, with a detector Monte Carlo. The same approach, however, does not fit the neutrino angular distribution well, which requires a better account for the geomagnetic effect. This is shown on Fig. 8, which compares data with calculated spread in terms of $\log(E/L)$ where L is the distance to the neutrino production point, taken to be at an altitude of 20 km and corresponding to a unique zenith angle. An isotropic distribution reverses the heights of the two peaks, which reflect the solid angle subtended.

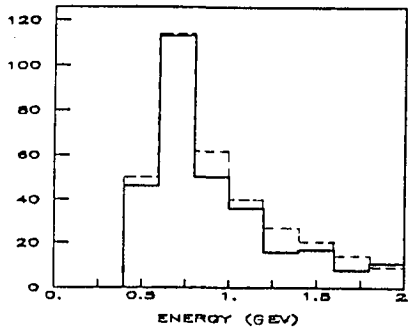

Fig. 7. Comparison of the measured neutrino energy spectrum for single-prong events (IMB) to a detector Monte Carlo (J. LoSecco) using the flux of Ref. 7(e).

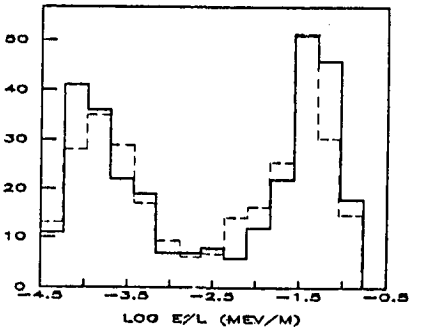

Fig. 8. Comparison of neutrino angular distribution (IMB) to the calculated in Ref. 7(e). No detector Monte Carlo. See text for definition of L.

The NUSEX detector is a cube of 3.5 m side and total mass of 150 tons. The active part of the detector consists of 43,000 plastic streamer tubes interspersed with 136 horizontal iron plates each 1 cm thick. Typical space resolution of the detector is 1 cm, but both resolution and trigger efficiency are anisotropic because of the horizontal arrangement. The operation time of the detector is 23,440 h, which gives a total exposure of 401 t/yr in which 31 contained events with visible energy $E_{vis} > 250$ MeV are detected. The neutrino rate, calculated with correction for the trigger and containment efficiency on an event-by-event basis, is 152 ± 20 ν/(kt.yr) and the ν_e/ν_μ ratio comes to a rather small value of 0.28 ± 0.11.

The apparatus of the Frejus group (fully completed in July 1985) is a big tracking detector with dimensions $6 \times 6 \times 12.3\,m^3$ and average density of 2.1 g/cm^3. A very high space resolution is achieved with 10^6 $0.5 \times 0.5\,cm^2$ flash tubes, triggered by 4×10^4 Geiger tubes. The arrangement of the sensitive and passive (1.5 mm thick iron plates) is vertical, so that the triggering efficiency is once again not isotropic. The neutrino statistics are collected with a fiducial mass of 585 tons and total exposure of 289 t.yr. A total of 22 neutrinos is observed, 14 of which are fully contained in the fiducial volume. Taking into account the average trigger and scanning efficiency this gives a rate of charge current events of 97 ± 25 ν/kt.yr. The observed ν_e/ν_μ ratio is 0.64 ± 0.30.

The prediction of Ref. 7(e) for both NUSEX and Frejus detectors, which are located nearby, is 120 ν/kt.yr for solar maximum, and the uncertainty of the calculation is at least 10%. The predicted ν_e/ν_μ ratio is 0.64.

To compare the results of NUSEX and Frejus one has first to substract the contamination of the neutral current, which from Frejus data is $\sim$ 15%, from the NUSEX rate. Then both rates agree within 1σ—a quite good agreement keeping in mind the difficulties in accounting for the efficiency and the difference in the way it is performed for the two experiments.

The difference in the measured ν_e/ν_μ ratio is more surprising. Apart from the low statistics, the efficiency for observing μ decays is low and the experiments have to rely on the shape of the track to distinguish between electrons and muons. There are some indications from the detector with higher resolution (Frejus) that some electron tracks at $E \sim 200$ MeV would look very much like muon tracks.[9] If some electron tracks were misinterpreted and counted as muons, this would cure not only the ν_e/ν_μ ratio, but also the apparent lack of low-energy electron neutrinos in the NUSEX energy spectrum.

The rate of contained events at KGF, as can be concluded from Fig. 1 of HE-6.2-3, is also in good agreement with their prediction for atmospheric neutrinos.

The conclusion, which can be drawn from the results on contained neutrino events, presented at this conference, is that all observations are compatible with the hypothesis that all observed neutrinos are of atmospheric origin. In addition to the rates, the analysis of the angular distribution, performed by J. LoSecco, shows that the account for the geomagnetic effect improves the agreement with data.

The statistics are, however, still low and the statistical errors alone give us room for some hopes for more exciting physics, some of which is contained in the next topic.

NEUTRINO FLUXES EXPECTED FROM EXTRATERRESTRIAL POINT SOURCES

The recent observations of γ rays with $E \geq 10^{15}$ eV from point sources[10] have increased the hopes for a working experimental neutrino astronomy. The idea has been suggested by different authors.[11] Cosmic-ray nuclei of very high energy interact within the clusters of matter, which we know exist in the universe, and produce neutrinos through the decay of the secondary particles. Only recently, however, we have observed γ rays with energy so high that the only reasonable production mechanism is $\pi^\circ \rightarrow 2\gamma$ decay and subsequent electromagnetic cascading. In a stellar environment a large fraction of the charged pions and kaons generated in the same interactions will necessarily decay and give rise to neutrinos.

Such neutrino fluxes are expected to be low and the only reasonable way of detection is the use of the Earth as a target for neutrino interactions. Only muons have long enough range to survive to the detectors and only the interaction $(\bar{\nu}_\mu) + N \rightarrow \mu + X$ is of practical interest. In order to calculate the observable quantity, which is the flux of neutrino-induced muons, one has to fold the neutrino flux dN_ν/dE_ν with the neutrino cross section $d\sigma/dE_\mu$ and integrate over the muon range. The double differential flux is[12]

$$\frac{dN_\mu}{dE_\mu dE_\nu} = \rho N_A \int_0^\infty dX \int_{E_\mu}^{E_\nu} dE'_\mu \, g(X, E_\mu, E'_\mu) \frac{d\sigma}{dE'_\mu} \frac{dN_\nu}{dE_\nu} ,$$

where $g(X, E_\mu, E'_\mu)$ is the probability that a muon generated with E'_μ will have energy E_μ after path X in rock. Three calculations of muon fluxes, induced by neutrinos from extraterrestrial point sources were presented at the conference.

Berezinsky, Castagnoli and Galeotti [HE 5.3-15/16] first calculated the neutrino production at a standard source. A standard source in their definition is a source of accelerated particles, embedded in a gas cloud of column density $x >> 70$ g/cm^2 and in the same time transparent to neutrinos. The flux of neutrino-induced muons is calculated from the neutrino flux at Earth using the average muon energy loss in rock and a neutrino cross section derived from the structure functions of Ref. 13.

The output from this calculation is the rate of muons with energy $> E_\mu$ in a 100 m^2 detector from a source of proton luminosity $L_p = 10^{43}$ erg/s at a distance 10 kpc as a function of the proton integral energy spectrum index γ. Table II shows some of the calculated rates for $E_\mu > 10$ GeV which depend very strongly on the value of γ.

Table II

$\gamma =$	1.1	1.2	1.4	1.6	1.8	3.0
$N_\mu(E > 10$ GeV)	1200	690	130	23	4.7	1.1

For sources at different distances and luminosities the calculated rates have to be appropriate scaled.

Gaisser and Stanev [HE 5.3-17] employ an entirely different approach. A model of the X-ray binary source[14] consisting of a pulsar and companion star is combined with a particular density model of the companion star, in which accelerated protons produce "star showers". The star properties vary with the phase and the neutrino attenuation in the star is accounted for. Fig. 9 shows a comparison of the neutrino flux from the source ($L_p = 10^{39}$ erg/s, $R = 10$ kpc) with the atmospheric ν_μ flux.

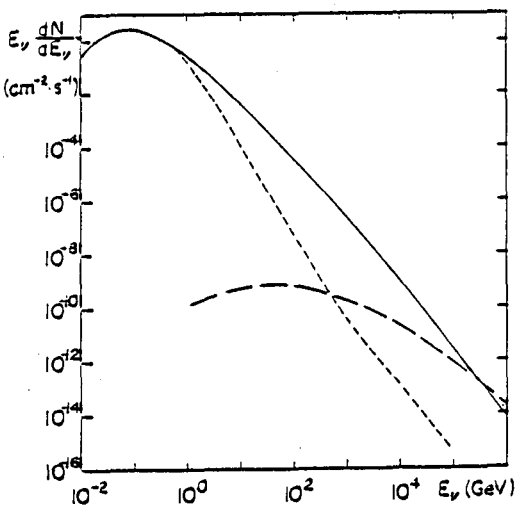

Fig. 9. Neutrino flux from Cygnus X=3 compared with the atmospheric flux (solid line). Dashed line is an estimate of the atmospheric background assuming detector resolution of 1°. For E_ν below about 1 TeV angular resolution is dominated by scattering angle in charged current neutrino interaction rather than by detector resolution.

Folded with the neutrino cross section (using two different structure functions) and muon propagation in rock the result for $\gamma = 1$ is

$$\text{Rate} = 10^{-3} \frac{L_{39}}{R_{10}^2} \text{ events/m}^2 \text{ yr}$$

and scales with the luminosity and the inverse square of the distance.

This rate is in agreement with the result of Berezinsky *et al.* for $\frac{1}{4}$ sr beaming of the proton beam and also with results of other recent calculations.[15] A remarkable consequence of the agreement between different calculations is that the expected neutrino-induced muon rate from point sources is not very sensitive to the conditions at the source. It confirms the conclusions of Ref. 16 that for target densities $< 10^{-6}$ g/cm^3 and thicknesses $\lesssim 100$ g/cm^2 the neutrino-induced muon rate varies only by factors of two or three. The new calculations also confirm the conclusions of Stenger[11] that the muon rate does not depend strongly on the muon detection threshold energy which favors large and not densely instrumented detectors such as DUMAND. The expected rates are very close to being observable by the proposed MACRO experiment [HE 6.1-4] with a sensitive area > 1000 m^2. Ten events per year in such a detector require for a source distance 10 kpc a proton luminosity $L_p > 10^{40}$ erg/s for 4π emission and correspondingly less if the emission is beamed.

In a related paper [HE 5.3-12] the MACRO collaboration has studied the detector response to point source neutrino fluxes and determined the minimum detectable neutrino flux as a function of the neutrino energy spectrum which for $\gamma = 1$ is 2.10^{-8} erg/cm^{-2} s^{-1}. The minimum detectable flux grows very rapidly with γ not only because of the importance of the production of high-energy (*i.e.* long-range) muons, but also because low-energy muons rapidly scatter out of the 1° cone, determined by the experimental resolution.

The location of the MACRO detector is suitable for observation of neutrino emission of X-ray binaries from the southern say, such as Vela X-1 and LMC X-4.

The general conclusion from the calculations of neutrino fluxes from X-ray binaries is that if the neutrino emission of these objects has a flat energy spectrum, similar to that of the observed UHE γ rays, weak signals from such objects are expected in 1000 m^2 detectors. This is especially true for faraway sources, such as LMC X-4 (estimated distance 50 kpc) whose γ-ray flux is degraded in interactions on the 3° background radiation.[17]

ACKNOWLEDGMENTS

This work was supported in part by the U. S. National Science Foundation and the U. S. Department of Energy under contract DE-AC02-76ER00881.

BRIEF NEWS

- Muon energy spectrum seems still quite steep above 1 TeV: $\gamma_{diff} \sim 4$ at Baksan [HE 5.1-15] and Artyomovsk [HE 5.1-6].
- Large surface-underground telescope is in operation at Homestake. A surface shower array will estimate shower energy, accompanying high-energy muons, and help with composition studies [HE 6.1-9].
- Muon photoproduction cross section may be a factor of 3 higher at $E_\mu \sim 10$ TeV [HE 5.4-12].
- New large liquid scintillation detector (90 tons) is operated in Mont Blanc Laboratory by INR (Moscow) and the Torino group [HE 5.3-6].
- Matter effects totally modify expectations for ν oscillations [HE 5.3-9/10].
- Testing continues at DUMAND. Important test with three detector strings (triad) is scheduled for 1986.
- No ν-induced (upward-going) air showers have been seen by the Fly's Eye above 10^{17} eV [HE 5.3-1].
- No evidence for ν oscillations from IMB data [HE 5.3-7].
- No young μ-poor showers at $\theta > 70°$ seen at Akeno—charm and heavier flavor cross section must be < 1 mb [HE 5.2-12].

REFERENCES

1. See, *e.g.*, J. Rushbrooke, talk at Inter. Europhysics Conf. on High Energy Physics, Bari, Italy, 1985, and UA5 talks at this conference.
2. T. K. Gaisser, Phys. Lett. B100, 425 (1981).
3. R. W. Clay, rapporteur talk at this conference.
4. J. Linsley, Proc. 18^{th} Inter. Cosmic Ray Conf., Bangalore, 1983, ed. by N. Durgaprasad *et al.* (Tata Institute of Fundamental Research, Bombay, 1983), vol. 12, p. 135.
5. For a description of the composition which fits data best, see G. G. Yodh *et al.*, Proc. ICOBAN '84, Park City, Utah, ed. by D. Cline (Univ. of Wisconsin, 1984).
6. J. W. Elbert, in Proc. DUMAND Summer Workshop, La Jolla, ed. by A. Roberts, (Scripps Institution of Oceanography, La Jolla, 1979), vol. 2, p. 101; T. K. Gaisser and T. Stanev, NIM, A235, 183 (1985).
7. (a) A. C. Tam and E.C.M. Young, in Proc. 11^{th} ICRC, Budapest, 1969, Acta Phys. Hung. 29, Suppl. 4, 307 (1970);

(b) E.C.M. Young, in *Cosmic Rays at Ground Level*, ed. by A. W. Wolfendale (Hilger, London, 1973), p. 105;
(c) J. L. Osborne, S. S. Said and A. W. Wolfendale, in Proc. Phys. Sco. London 86, 93 (1976);
(d) L. V. Volkova, Yad. Fiz. 31, 1510 (1980)[Sov. J. Nucl. Phys. 31, 784 (1980)];
(e) T. K. Gaisser *et al.*, Phys. Rev. Lett. 51, 223 (1983); T. K. Gaisser and T. Stanev, in Proc. SWOGU, Minneapolis, 1985, ed. by S. Rudaz and T. Walsh, in press.

8. Details of conversion from visible lepton energy are given in J. M. LoSecco *et al.*, Phys. Rev. Lett. 54, 2299 (1985).
9. B. Degrange and F. Raupach, private communication (1985).
10. For the most recent review, see A. A. Watson's rapporteur talk at this conference.
11. See, *e.g.*, D. Eichler, Nature 275, 725 (1978); V. S. Berezinsky, in Proc. DUMAND Summer Workshop, 1979, ed. by L. Learned; V. J. Stenger, Ap. J. 284, 810 (1984) and references therein.
12. T. K. Gaisser and T. Stanev, Phys. Rev. 30, 985 (1984).
13. D. W. Duke and J. J. Owens, Phys. Rev. 30, 49 (1984).
14. W. T. Vestrand and D. Eichler, Ap. J. 261, 251 (1982).
15. E. W. Kolb, M. S. Turner and D. W. Walker, Phys. Rev. 32, 1145 (1985); G. Auriemma, H. Bilokon and A. F. Grilo, in Underground Physics '85, St. Vincent, Italy, 1985.
16. T. K. Gaisser and T. Stanev, Phys. Rev. Lett. 54, 2265 (1985).
17. G. Cocconi, CERN preprint, 1985; T. K. Gaisser, in New Particles '85, Madison, ed. by V. Barger, D. Cline and F. Halzen.